Towards an improved magnetic diagnostic system for *LISA*

Journal of Physics: Conference Series **154** (2009) 012005 doi:10.1088/1742-6596/154/1/012005

Towards an improved magnetic diagnostic system for *LISA*

I Mateos[1], A Lobo[1], J Ramos-Castro[2], J Sanjuán[1] and M Nofrarias[3]

[1] Institut de Ciències de l'Espai (CSIC-IEEC), Edifici Nexus, Gran Capità 2-4, 08034 Barcelona, Spain

[2] Departament d'Enginyeria Electrònica, Universitat Politècnica de Catalunya (UPC), Campus Nord, Edifici C4, Jordi Girona 1-3, 08034 Barcelona, Spain

[3] Max-Planck-Institut für Gravitationsphysik (Albert-Einstein-Institute), Callinstrasse 38, D-30167 Hannover, Germany

E-mail: mateos@ice.csic.es

Abstract. The current design, and material implementation of the magnetic field sensing in the *LISA* Technology Package (*LTP*) on board *LISA* Pathfinder (*LPF*), is based on a set of 4 high-precision 3-axis fluxgate magnetometers. In order to avoid magnetic disturbances on the *LTP* proof masses (*TM*'s), originated by the sensors themselves, these are placed somewhat far from the *TM*'s, which results in partial field information losses. We are currently investigating alternative magnetic sensing techniques, based on *AMR* (Anisotropic Magnetoresistive) devices. These are much smaller in size than fluxgates, therefore a more numerous array can be thought of for flight. In addition, there is a chance that they may be attached closer to the *TM*'s, thereby enhancing magnetic field sensing spacial resolution. Several issues need to be addressed, such as real sensitivity (including electronics noise) and set/reset trigger procedures. A brief overview about the stability of the magnetic fields and gradients generated in the *LTP* by means of the coil will also be given. This paper show the latest results of our research.

1. Introduction

LISA Pathfinder [1] is a technologically sophisticated Mission to demonstrate that two proof masses can be put into free-fall to a certain level of accuracy. This idea is reflected in the differential acceleration noise requirements for the *LTP*

$$S^{1/2}_{\delta a,\mathrm{LPF}}(\omega) \leq 3\times 10^{-14}\left[1+\left(\frac{\omega/2\pi}{3\ \mathrm{mHz}}\right)^2\right]\mathrm{ms}^{-2}\mathrm{Hz}^{-1/2} \quad (1)$$

in the frequency band between 1 mHz and 30 mHz. *LISA* has a increased acceleration noise budget ($3\,\mathrm{fms}^{-2}\mathrm{Hz}^{-1/2}$) in the frequency band between 0.1 mHz and 0.1 Hz. This noise is the result of various disturbances which limit the performance of the instrumentation on-board. Magnetic disturbances are foreseen to contribute a significant fraction of the total acceleration budget. The effect of magnetic disturbances takes places as a consequence of the magnetic properties of the test masses, more precisely their remmant magnetic moment ($\mathbf{m}_0$) and their magnetic susceptibility (χ). Therefore, magnetometers have been required to be embarked with the purpose to produce an as accurate as possible map of magnetic field and gradient in the region of the *TM*s and also a pair of coaxial magnetic coils will generate controlled magnetic

fields, which add linearly to the environmental one and gives rise to a total force per TM given by

$$F_x = \left\langle \left[\left(\mathbf{M} + \frac{\chi}{\mu_0} \mathbf{B} \right) \cdot \nabla \right] B_x \right\rangle V \tag{2}$$

These coils are intended to perform in flight measurements of $\mathbf{m}_0$ and χ, which will assess eventual deviations of the values of these parameters (measured in ground) generated during launch.

1.1. Magnetic Field Measurements

The magnetometers used in *LISA* Pathfinder are fluxgate type (Billingsley TFM100G4-VQS) —see figure 1. These magnetometers are able to perform very low noise measurements in the bandwidth between 1 mHz and 30 mHz, however, they are bulky and present other disadvantages such as:

- The spatial resolution of the magnetic field measurement is limited due to the large head sensor.
- They need to be placed far from the *TM*'s due to the quantity of permalloy (nickel-iron) contained in the fluxgate's core that can provoke magnetic disturbances in the *TM*'s.

In order to overcome the above limitations, we have done some preliminary research to assess the performance of another type of magnetometer, Anisotropic Magnetoresistive (*AMR*) sensors —see figure 1, in the *LTP* and *LISA* measurement bandwidth (*MBW*).

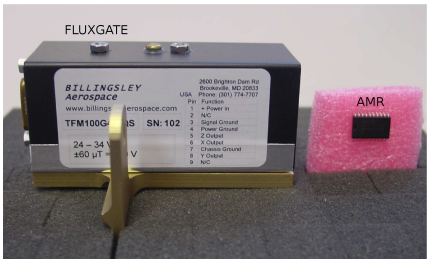

Figure 1. Left: Billingsley fluxgate magnetometer. Right: Honeywell *AMR* magnetometer.

1.2. Magnetic Fields and Magnetic Field Gradients Generation

Stability of the magnetic field and gradients created by the coils must comply with requirements [1] depending on the *TM*'s distance. This stability is required in order to determine accurately the magnetic properties of the *TM*'s (($\mathbf{m}_0$ and(χ)). The stability of the created magnetic field is equivalent to the stability of the driving current, hence the requirement can be expressed in terms of the current fluctuation of the current source —see table 1.

Table 1. Requirements of the magnetic field produced by the coils in the *LTP MBW*.

Magnitude		$S_I^{1/2}$
$S_{B_z}^{1/2}$	5 nT/$\sqrt{\text{Hz}}$	1.12 μA/$\sqrt{\text{Hz}}$
$S_{\partial B_z/\partial x}^{1/2}$	12 nT/m/$\sqrt{\text{Hz}}$	110 nA/$\sqrt{\text{Hz}}$

2. Magnetic field measurement

2.1. Proposal Front-End Electronics for the AMR

The analog signal conditioning circuit for the magnetic field sensing is shown in figure 2. A Wheatstone bridge is powered with an ac square signal ($f_{\rm B} \approx 5$ Hz). This switching reduces the $1/f$ noise of the Instrumentation Amplifier (IA) by modulating the low frequency signals of interest to a higher band. The output signal from the bridge is amplified, low-pass filtered and sampled [2]

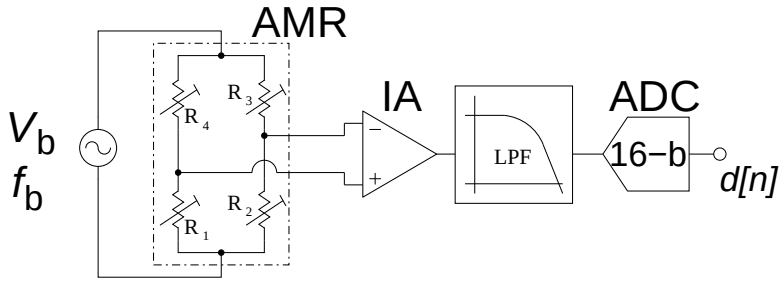

Figure 2. Analog signal processing scheme.

The resistance-magnetic field dependence of the AMR can be modeled as [3]:

$$R(H_y) = R_0 + \Delta R \frac{H_y}{H_0}\sqrt{1-\left(\frac{H_y}{H_0}\right)^2} \tag{3}$$

where H_0 is the total anisotropic field, H_y is the measured field (perpendicular to the easy-axis), $R_0 \simeq 850\,\Omega$ is the nominal resistance of the AMR. The output voltage of the four sensor Wheatstone bridge can be described by:

$$V_{\rm o} = V_{\rm B}\frac{\Delta R}{R_0}\frac{H_y}{H_0}\sqrt{1-\left(\frac{H_y}{H_0}\right)^2} \tag{4}$$

where $V_{\rm B} = 5$ V is the bridge voltage excitation. Therefore the sensitivity ($dV_{\rm o}/dH_y$) of the bridge is $s_{\rm B} = \frac{\Delta R}{R_0}\frac{V_{\rm B}}{H_0} = 160\mu{\rm V}/\mu{\rm T}$, in the temperature range of -25 to 100 °C. The gain of the IA has been set to 200, therefore the *global* sensitivity is $s_{\rm total} = s_{\rm B}\cdot G_{\rm IA} = 32\,{\rm mV}/\mu{\rm T}$.

Once the signal has been sampled by the analog-to-digital converter (ADC), the digital demodulating process begins. This process is shown in figure 3 and it consists, basically, on a decimator and a subsequent difference averaging.

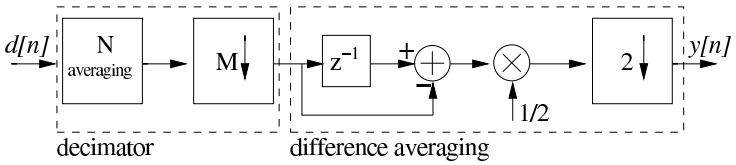

Figure 3. Digital de-modulation process.

2.2. Noise density in the AMR sensor

The total noise of the measurement chain, $S_H^{1/2}$, in terms of magnetic field spectral density can be written as:

$$S_H^{1/2}(H,\omega) = [S_{H,\mathrm{B}}(H,\omega) + S_{H,\,IA}(H,\omega) + S_{H,\,ADC}(H,\omega)]^{1/2} \tag{5}$$

where (all the terms are in $\mathrm{T/Hz^{1/2}}$ units):

- $S_{H,\,\mathrm{B}}(H,\omega)$ is the bridge noise density
- $S_{H,\,IA}(H,\omega)$ is the *IA* noise density refered to the input
- $S_{H,\,ADC}(H,\omega)$ is the *ADC* noise density refered to the input

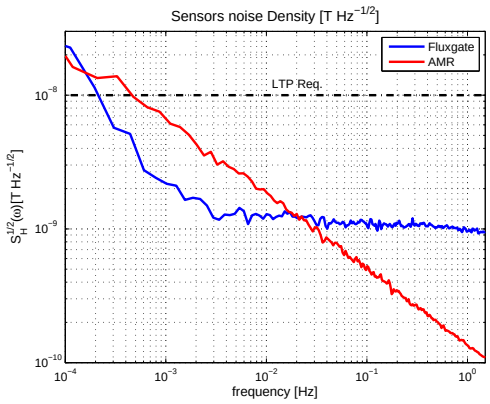

Figure 4. Magnetic field noise density for Fluxgate (blue) and *AMR* (red) sensors.

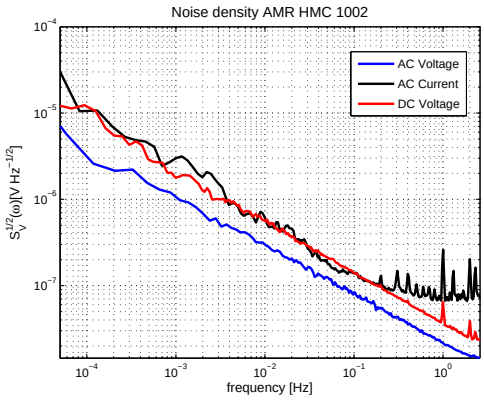

Figure 5. Voltage Noise density of the *AMR* with different Wheatstone Bridge excitation schemes. AC Voltage= 5 V, AC Current= 10 mA, DC Voltage=5 V.

Measurements using flux-gate and AMR magnetometers are shown in Figure 4 where it can be noticed that the magnetic field noise for both sensors is similar at the frequencies of interest for *LISA* (0.1 mHz). Between 1 mHz and 30 mHz both are below the *LTP* requirements. Above 20 mHz the differences are due to the measurement resolution, both have a 16 bits *ADC*, however, in the digital processing of the *AMR* the samples are averaged ($N = 3072$) and, thus, an equivalent resolution of 22 bits ($16 + \frac{1}{2}\log_2 N$) is obtained.

2.3. Magnetic characterisation of the AMR

AMR sensors are made of a nickel-iron thin film deposited on a silicon wafer and is patterned as a resistive strip. These materials can show ferromagnetic behaviours (except Silicon that shows diamagnetism) and could be potentially dangerous if they are to be attached near the test mass. Moreover the *AMR* film properties are well behaved only when the film's magnetic domains are aligned in the same direction (material saturated).

Most low field magnetic sensors will be affected by a large magnetic disturbing field ($>300\,\mu$T) that may lead to output signal degradation. This disturbing field actually breaks down the magnetisation alignment in the Permalloy film. In order to reduce this effect, a large current Set/Reset pulse can be applied during $\simeq 2\mu$s to eliminate the effect of past magnetic history.

The state of these magnetic domains can retain for years as long as there is no magnetic disturbing field present ($\simeq 6 \cdot H_{\mathrm{Earth}}$).

Due to the strong magnetic requirement [1] of the mission —see table 2, the magnetic moment of the *AMR* HMC1001 was measured in a SQUID (Quantum Design MPMS XL Squid). We are interested in the saturation magnetic moment because it will be the normal operation state of the *AMR*.

Table 2. Magnetic requirements in the *LTP*

Magnitude	dc Req.	PSD Req.
B_z	10 μT	650 nT/$\sqrt{\mathrm{Hz}}$
$\partial B_z/\partial x$	5 μT/m	250 nT/m/$\sqrt{\mathrm{Hz}}$

The measured hysteresis curve (see Figure 6) shows a saturation magnetic moment of $m_{\mathrm{sat}} \simeq 0.44\ \mu\mathrm{Am}^2$, more than an order of magnitude below the remanent magnetic moment of the *NTC* ($m_{\mathrm{r}} \simeq 26\,\mu\mathrm{Am}^2$) placed in the electrode housing of the *LTP* and at a distance of $\simeq 13$ mm of the *TM* [4].

In order to estimate the magnetic field and magnetic field gradient caused by the *AMR* we shall make the assumptions that the sensors behave like magnetic dipoles. Figure 7 shows magnetic field and magnetic field gradient created by a *AMR* are within the requirements.

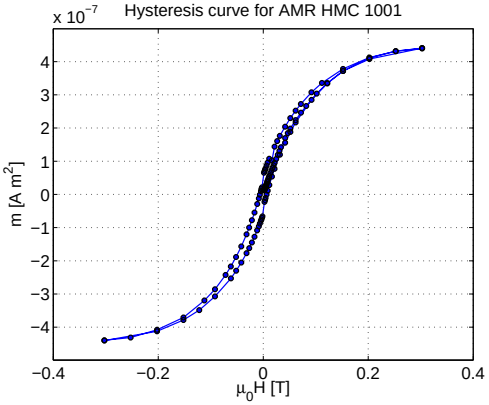

Figure 6. Hysteresis curve at 300 K for the *AMR*.

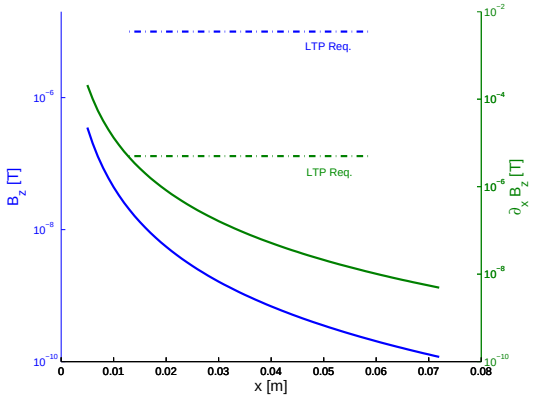

Figure 7. Magnetic field (blue) and magnetic field gradient (green) created by a *AMR*.

3. Controlled magnetic excitations: Coil current stability

Different current source topologies [5] have been tested at *LISA* Bandwidth, obtaining the best result with the *floating load current source*, although the *differential current source* topology could be a good option, within the requirements —see table 3.

Table 3. Noise density results for different current sources typologies.

Typology	1 mHz			0.1 mHz		
	$S_I^{1/2}$ $\left[\frac{\text{nA}}{\sqrt{\text{Hz}}}\right]$	$S_B^{1/2}$(*) $\left[\frac{\text{pT}}{\sqrt{\text{Hz}}}\right]$	$S_{\partial B/\partial x}^{1/2}$ (*) $\left[\frac{\text{nT}}{\text{m}\sqrt{\text{Hz}}}\right]$	$S_I^{1/2}$ $\left[\frac{\text{nA}}{\sqrt{\text{Hz}}}\right]$	$S_B^{1/2}$(*) $\left[\frac{\text{pT}}{\sqrt{\text{Hz}}}\right]$	$S_{\partial B/\partial x}^{1/2}$(*) $\left[\frac{\text{nT}}{\text{m}\sqrt{\text{Hz}}}\right]$
Floating load	6	26.8	0.65	34	152	3.71
Differential	17	76	1.86	80	357.8	8.74
Howland	50	223.6	5.46	210	939.2	22.94

(*) To estimate $S_B^{1/2}$ and $S_{\partial B/\partial x}^{1/2}$ have been assumed a coil's mean radius of 56.5 mm and a distance *TM* center-Coil center of 85.5 mm (Actual *LTP* configuration)

Figure 8 shows the theoretical [6] and measured current stability in the *Floating load* topology, dominated by the $1/f$ noise. The magnetic field gradient noise density obtained with this current pump at *LISA* Bandwidth (0.1 mHz) is shown in figure 9, where x is the distance of the TM from the coil and ρ is the distance from the axis of the coil.

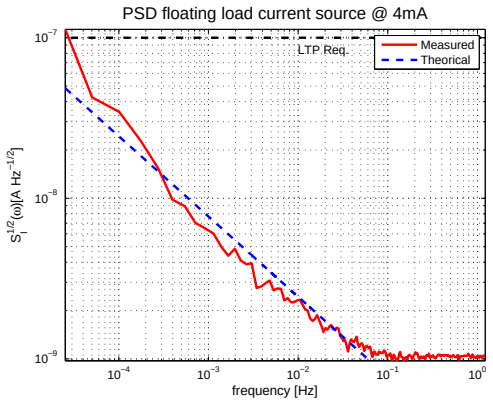

Figure 8. Current noise density of the *Floating load* current pump.

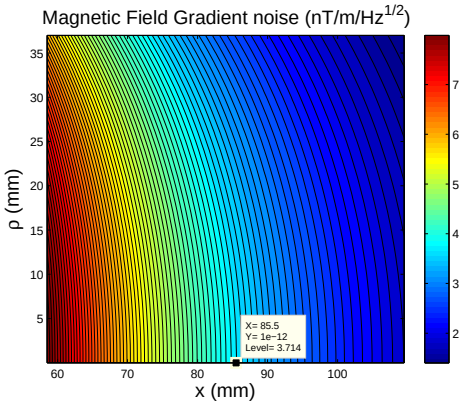

Figure 9. $S_{\partial B/\partial x}^{1/2}$: Magnetic field gradient noise. Label points out the *TM* centre.

4. Conclusions

AMR magnetometers sensors are smaller and present lower power consumption than fluxgate magnetometers, hence, higher spatial resolution with less power consumption is attainable. In addition, we have shown that the measurement noise levels requirement are also fulfilled when using *AMR* sensors in the *LTP* bandwidth and near to the requirement in the frequency of interest of *LISA*. Moreover, the very low magnetisation of the *AMR* sensors allows to place the sensors very close to the *TM*'s and, in consequence, an accurate measurement of the magnetic field in the *TM*'s can be made. For these reasons *AMR* magnetometers appear as a solution to the magnetic field measurement in the *LISA* mission. We also have shown that the *floating load current source* topology fulfils clearly the coil current stability requirements in the *LISA* bandwidth.

Acknowledgments
We wish to thank Núria Clos for her excellent work at the Serveis Científico-técnics of the Universitat de Barcelona and Ivan Lloro, Institut de Ciències de l'Espai, for his great help in managerial affairs. Support for this work came from Project No. ESP2004-01647 of Plan Nacional del Espacio of the Spanish Ministry of Education and Science (MEC).

References

[1] Vitale S 2005 Science Requirements and Top-level Architecture Definition for the *LISA* Technology Package (*LTP*) on Board *LISA* Pathfinder (*SMART-2*), report no. LTPA-UTN-ScRD-Iss003-Rev1
[2] Sanjuán J, Lobo A, Nofrarias M, Ramos-Castro J and Riu P J. 2007 Thermal diagnostics front-end electronics for *LISA* Pathfinder *Rev. Sci. Instrum.* 78 104904
[3] Hauser H, Stangl G, Fallmann W, Chabicovsky R and Riedling K 2000 *Proc. Workshop Preparation, Properties, and Applications of Thin Ferromagnetic Films (Viena)* pp 15-27
[4] Sanjuán J, Lobo A, Nofrarias M, Ramos-Castro J, Mateos I and Xirgu X 2008 Magnetic polarisation effects of temperature sensors and heaters in *LISA* Pathfinder *Rev. Sci. Instrum.* 79 084503
[5] Franco S 2002 *Design with Operational Amplifiers and Analog Integrated Circuits* (London: McGraw-Hill)
[6] Pallàs R and Webster JG 1999 *Sensors and Signal Conditioning* (New York: Wiley-Interscience)